JGR Atmospheres

RESEARCH ARTICLE
10.1029/2018JD030127

Importance of Surface Roughness for the Local Biogeophysical Effects of Deforestation

J. Winckler, C. H. Reick[1], R. M. Bright[3], and J. Pongratz[1,4,2]

[1]Max Planck Institute for Meteorology, Hamburg, Germany, [2]International Max Planck Research School on Earth System Modeling, Hamburg, Germany, [3]The Norwegian Institute of Bioeconomy Research, As, Norway, [4]Department of Geography, Ludwig-Maximilians-Universität München, Munich, Germany

Abstract Deforestation influences surface properties such as surface roughness, resulting in changes in the surface energy balance and surface temperature. Recent studies suggest that the biogeophysical effects are dominated by changing roughness, and it remains unclear whether this can be reconciled with earlier modeling studies that highlighted the importance of a reduction of evapotranspiration in the low latitudes and a reduction of net shortwave radiation at the surface in the high latitudes. To clarify this situation, we analyze the local effects of deforestation on surface energy balance and temperature in the MPI-ESM climate model by performing three separate experiments: switching from forest to grass *all* surface properties, only surface albedo, and only surface roughness. We find that the locally induced changes in surface temperature are dominated by changes in surface roughness for the annual mean, the response of the diurnal amplitude, and the seasonal response to deforestation. For these three quantities, the results of the MPI-ESM lie within the range of observation-based data sets. Deforestation-induced decreases in surface roughness contribute substantially to winter cooling in the boreal regions and to decreases in evapotranspiration in the tropics. By comparing the energy balance decompositions from the three experiments, the view that roughness changes dominate the biogeophysical consequences of deforestation can be reconciled with the earlier studies highlighting the relevance of evapotranspiration.

Key Points:
- Climate model simulations reveal that surface roughness dominates the local surface temperature change signal in most geographic regions
- The study reconciles findings from studies focusing on changes in the surface energy balance and on changes in surface properties
- Model outcomes are consistent with observed changes in surface temperature across annual, diurnal, and seasonal time scales

Supporting Information:
- Supporting Information S1

Correspondence to:
J. Pongratz,
julia.pongratz@geographie.uni-muenchen.de

Citation:
Winckler, J., Reick, C. H., Bright, R. M., & Pongratz, J. (2019). Importance of surface roughness for the local biogeophysical effects of deforestation. *Journal of Geophysical Research: Atmospheres*, *124*, 8605–8618. https://doi.org/10.1029/2018JD030127

Received 16 JAN 2019
Accepted 14 JUL 2019
Accepted article online 20 JUL 2019
Published online 14 AUG 2019

Author Contributions
Conceptualization: J. Winckler, C. H. Reick, J. Pongratz
Funding Acquisition: J. Pongratz
Methodology: J. Winckler, C. H. Reick, J. Pongratz
Writing - Original Draft: J. Winckler
Formal Analysis: J. Winckler
Investigation: J. Winckler
Project Administration: J. Pongratz
Supervision: C. H. Reick, J. Pongratz
Writing - review & editing: J. Winckler, C. H. Reick, R. M. Bright, J. Pongratz

1. Introduction

Deforestation not only releases large amounts of carbon into the atmosphere (Le Quéré et al., 2018) but also influences the surface properties such as surface albedo, surface roughness, and evapotranspiration efficiency (defined as the ability of the land surface to transfer water to the atmosphere; Davin & de Noblet-Ducoudré, 2010). Changes in these surface properties alter the exchange of heat, moisture, and momentum between the surface and the atmosphere. It is important to understand the mechanisms by which the changes in the surface properties influence climate, because forest management practices (Anderson et al., 2010) or geoengineering strategies (Davin et al., 2014; Seneviratne et al., 2018; Thiery et al., 2017) may be designed to alter single surface properties in order to influence climate, in particular surface temperature.

When analyzing the mechanisms underlying deforestation, one must differentiate between surface properties and components of the surface energy balance (Figure 1). Locally, deforestation leads to a change in surface properties, for example, surface albedo may increase when forest is replaced by brighter grassland. The changes in surface properties then translate into changes in the surface energy balance (e.g., less net shortwave radiation absorbed by the surface, but also changing the latent and sensible heat fluxes) and finally changes in surface temperature at the location of deforestation (Figure 1). The changes in components of the surface energy balance and surface temperature that are triggered locally at a location of deforestation are henceforth referred to as the "local effects." Furthermore, changes in the physical state of the surface may affect the atmospheric conditions such as clouds (e.g., Teuling et al., 2017) and also atmospheric temperature and humidity (e.g., Davin & de Noblet-Ducoudré, 2010). Through changes in heat, moisture, and momentum advection (e.g., Khanna et al., 2017; Khanna & Medvigy, 2014), the changes in the atmosphere may be seen not only at the location of deforestation but also at locations that were not deforested (e.g., Avissar & Werth, 2005; Badger & Dirmeyer, 2016), thus resulting in changes in the surface energy balance at these locations. These remote changes, which are uncertain and can be challenging to

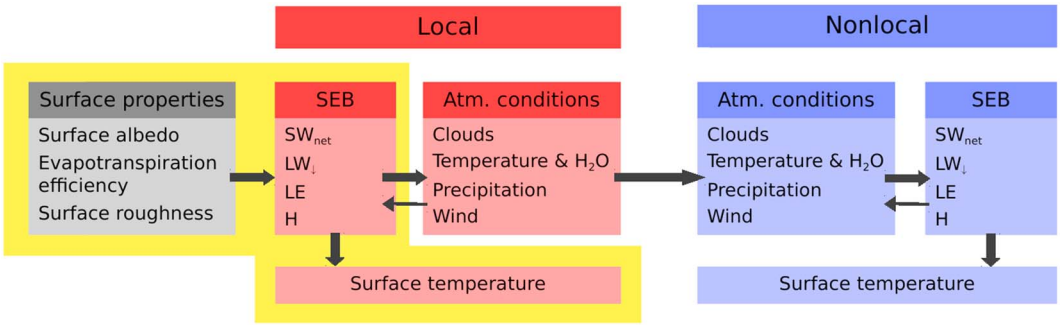

Figure 1. Illustration of how surface temperature is influenced by deforestation. At the location of deforestation, changes in surface properties translate into changes in the surface energy balance (SEB), and these result in changes in the surface temperature ("local effects"). The changes in the local surface energy balance can trigger changes in the atmospheric conditions, and these can also propagate to locations without deforestation, influencing the surface energy balance and the surface temperature there ("nonlocal effects"). The focus of this study (indicated by yellow) is the relation between changes in surface properties and resulting local effects on the surface energy balance and the surface temperature.

detect statistically (Lorenz et al., 2016), are henceforth referred to as "nonlocal effects." While the nonlocal effects may dominate the global mean response of surface temperature (Winckler, Reick, Lejeune, et al., 2019), this study focuses on the *local* biogeophysical effects for three reasons: (1) In contrast to the nonlocal effects, the local effects on surface temperature within a grid cell are largely independent of the spatial extent and location of deforestation elsewhere (Winckler et al., 2017a). Thus, the focus on the local effects enables process understanding that is independent of (to some extent arbitrary) choices of deforestation scenarios such as historical deforestation, possible future deforestation/afforestation or idealized large-scale deforestation/afforestation that alter not only local but also large-scale conditions like the background climate. (2) The local effects on surface temperature are relevant for forest- and other land-based strategies that aim at locally adapting to a warming climate. (3) The local effects in the climate model are relevant for the comparison with, and the interpretation of, observation-based data sets because these observation-based data sets by construction exclude any nonlocal effects (Alkama & Cescatti, 2016; Bright et al., 2017; Duveiller et al., 2018a; Li et al., 2015).

Previous studies that aimed at understanding the mechanisms that are responsible for deforestation-induced changes in surface temperature can be grouped into two kinds of studies: The first kind of studies focused on changes in the components of the surface energy balance. A satellite-based study showed that, concerning the local effects, deforestation in high latitudes leads to a surface cooling due to a reduction in net shortwave radiation at the surface, although some of this cooling is balanced by a reduced loss of sensible heat from the surface to the atmosphere (Duveiller et al., 2018b). Furthermore, the local effects of deforestation in lower latitudes lead to a surface warming due to a reduction in evapotranspiration and hence latent heat flux (Duveiller et al., 2018b). Concerning the total (local + nonlocal) effects, these ideas were already presented in climate modeling studies on idealized global-scale deforestation (e.g., Bala et al., 2007; Bathiany et al., 2010; Claussen et al., 2001; Devaraju et al., 2018), which argued that the boreal cooling is caused by a decrease in shortwave radiation and the tropical warming is caused by a decrease in evapotranspiration. Some observational and climate modeling studies also quantified how changes in the different terms of the surface energy balance contributed to changes in surface temperature by an explicit decomposition the surface energy balance (section 2) for deforestation (e.g., Boisier et al., 2012; Vanden Broucke et al., 2015; Winckler et al., 2017a). While these studies provide valuable information about deforestation-induced changes in the surface energy balance, neither the observation-based nor the model-based studies investigated which surface property is responsible for the analyzed changes in surface energy balance components.

A second type of studies used climate models in order to address this question of attribution of changes in surface temperature to changes in particular surface properties (surface albedo, surface roughness, and evapotranspiration efficiency; changes in evapotranspiration efficiency may be caused by changes in, e.g., leaf area index, rooting depth, and canopy conductance). For this attribution, simulations were performed in which only one surface property at a time was switched from forest to grass values (e.g., Bell et al., 2015; Charney et al., 1977; Davin & de Noblet-Ducoudré, 2010; Li et al., 2016; Polcher, 1995; Sud et al., 1988).

Studies using simulations in which only surface roughness was changed found that surface roughness can substantially influence atmospheric conditions. For instance, a decrease in surface roughness can increase wind speed and lead to changes in circulation (e.g., Sud & Smith, 1985; Sud et al., 1988) or trigger hydroclimatic changes such as a redistribution of rainfall (Khanna & Medvigy, 2014; Khanna et al., 2017; Sud et al., 1988). On the other hand, simulated changes in surface albedo were found to substantially influence temperature (Charney et al., 1977; Davin et al., 2014). Concerning changes in surface temperature due to global-scale deforestation, the study by Davin and de Noblet-Ducoudré (2010) found that changes in surface albedo (leading to strong global cooling) dominate changes in evapotranspiration efficiency and surface roughness (leading to warming). However, due to the large scales at which the surface properties in these studies are changed, the changes in surface temperature in their studies may be dependent on the presence of strong nonlocal effects, which are the main pathway for the albedo-induced change in surface temperature (Winckler, Reick, Lejeune, et al., 2019). Thus, it still remains unknown which surface property was responsible for the changes in surface temperature due to deforestation with regards to the local effects. For an improved understanding on how deforestation leads to changes in biophysical conditions, it would be desirable to link more directly the studies focusing on the surface energy balance, for example by a surface energy balance decomposition, and the studies altering individual surface properties—the latter studies focused predominantly on changes in surface temperature, with little quantitative information on changes in the terms of the surface energy balance. It seems intuitive to interpret high-latitude cooling associated with reduced shortwave absorption as attributable to albedo changes, or tropical warming associated with reduced evapotranspiration as attributable to changes in evapotranspiration efficiency. However, for instance, changes in evapotranspiration may also be substantially influenced by changes in surface roughness (Dickinson & Henderson-sellers, 1988), and thus, this attribution of changes in surface energy balance components to changes in surface properties is not unique.

Another way to attribute the deforestation-induced changes in surface temperature to physical mechanisms was developed by Juang et al. (2007). They derived analytical expressions to attribute the surface temperature response (mainly due to local effects) to changes to specific "ecophysiological" or "intrinsic biophysical mechanisms" (IBPMs). Such expressions have recently been applied to analyze climate model output (Burakowski et al., 2018; Chen & Dirmeyer, 2016; Devaraju et al., 2018; Rigden & Li, 2017) or in situ observations (Bright et al., 2017; Juang et al., 2007; Lee et al., 2011; Liao et al., 2018). Changes in surface temperature were attributed to a "surface albedo" term and an "energy redistribution" term (Lee et al., 2011), which is often divided in an "aerodynamic resistance term" (or "roughness term") and either a "bowen ratio term" (Lee et al., 2011) or "surface resistance term" (Liao et al., 2018; Rigden & Li, 2017). These studies found that the roughness term dominates the locally induced changes in surface temperature. However, the roughness and bowen ratio terms are not independent of each other (Liao et al., 2018; Rigden & Li, 2017), and thus, it is unclear how these terms (e.g., roughness term) relate to the surface properties (e.g., "surface roughness") whose influence was investigated in the climate models. In addition, the IBPM terms may include other interactions between the albedo, bowen ratio and roughness terms. For instance, an isolated change in surface albedo in a model may influence the amount of shortwave net radiation at the surface. This may influence latent and sensible heat fluxes differently (e.g., in a water-limited region) and thus lead to a change also in the bowen ratio, so the "albedo" term in the study by Lee et al. (2011; comprising only changes in shortwave net radiation) may not be conceptually identical with the changes that would be triggered by changing surface albedo in a climate model (comprising also changes in latent and sensible heat fluxes).

The importance of the roughness term in the IBPM studies seems to suggest that surface roughness is important not only for the total (local + nonlocal) biogeophysical deforestation effects (e.g., Dickinson & Henderson-sellers, 1988; Khanna & Medvigy, 2014; Sud et al., 1988) but also for the locally induced changes in surface temperature. The importance of the roughness term in the IBPM studies, both for deforestation-induced high-latitude cooling and low-latitude warming, seems to contradict climate modeling studies that focus on changes in the surface energy balance components, which highlight the importance of a reduction of shortwave radiation for the high-latitude cooling and a reduction of latent heat (evapotranspiration) for low-latitude cooling (e.g., Claussen et al., 2001; Bathiany et al., 2010; Devaraju et al., 2015). Our research question is whether these findings are indeed contradictory, or whether the apparent discrepancies can be explained by (1) the presence of nonlocal effects (mainly excluded in the IBPM method but included

in most climate modeling studies) or (2) a different focus of the studies (changes in surface properties vs. changes in surface energy fluxes).

To address this question, we focus our analysis on the local effects. This allows us to assess whether looking at total (local + nonlocal) versus local effects can reconcile previous studies. We perform simulations with the climate model MPI-ESM and contrast the effects on the surface energy balance when concurrently changing all surface properties that are affected by deforestation (surface albedo, surface roughness, and evapotranspiration efficiency) with the effects of only changing surface roughness and only changing surface albedo. By changing only surface roughness, we are able to isolate the aerodynamic controls on the surface energy balance from the purely physiological controls (e.g., leaf stomatal control on transpiration). The presented analysis relies on a single climate model. In order to check whether the model yields reasonable results, we compare the MPI-ESM results against observation-based data sets for changes surface temperature at diurnal, seasonal and annual time scales.

2. Methods

2.1. Surface Properties in the MPI-ESM Model

Simulations are preformed using the climate model MPI-ESM (Giorgetta et al., 2013), which has been evaluated with respect to key characteristics that are essential in representing the deforestation effects, including surface albedo (Boisier et al., 2013; Brovkin et al., 2013), hydrology (Loew et al., 2013; Zhang et al., 2017), evapotranspiration (Boisier et al., 2014), and soil moisture-climate feedbacks (Berg et al., 2016; Seneviratne et al., 2013). In addition, previous studies compared the biogeophysical effects of land cover change in the MPI-ESM to other models (Brovkin et al., 2013; de Noblet-Ducoudré et al., 2012; Pitman et al., 2009) and satellite-based observations (Duveiller et al., 2018).

Central to this study are surface albedo and surface roughness. In the MPI-ESM, surface albedo is calculated separately for near-infrared and visible solar radiation. The albedo of a grid box is combined from contributions of ground, leaf albedo (distinguishing between different plant functional types), and snow. The leaf area index of the respective plant functional type is accounted for (see Table 1), as well as the masking of the underlying snow by the vegetation canopies under forests. More details on the calculation of land surface albedo for snow-free and snow-covered areas can be found in the studies by Otto et al. (2011) and Dickinson et al. (1993), respectively. Deforestation in the MPI-ESM results in a change in surface albedo of around 5–10% in snow-free areas but can reach values of around 20–30% in areas with seasonal snow cover. A map of the deforestation-induced yearly average changes in surface albedo is shown in Figure S1 in the supporting information.

The roughness length of vegetated surfaces is calculated separately for each plant functional type i and is interpolated between two roughness length values $z^i_{0,\Lambda=0}$ and $z^i_{0,\Lambda=\infty}$ (see Table 1), the first representing the value in the absence of leaves, and the second the one for a closed canopy, where Λ is the leaf area index. Using these two values, the roughness length of plant functional type i is calculated as

$$z^i_0 = z^i_{0,\Lambda=0} + (z^i_{0,\Lambda=\infty} - z^i_{0,\Lambda=0}) \tanh(\gamma\Lambda), \tag{1}$$

where the parameter γ (here $\gamma = 0.4$) controls how fast the roughness length saturates with increasing leaf area index. For the calculation of the latent and sensible heat fluxes within a grid cell, surface roughness is aggregated from the different subgrid vegetation tiles and bare soil using the blending height concept (Claussen, 1995).

2.2. Simulation Setup

Simulations with the MPI-ESM are performed using a horizontal atmospheric resolution of about 1.9° with atmospheric CO_2 concentrations prescribed at a preindustrial level. After a spin-up of 150 years, 200 years is analyzed. The analyzed variables (surface temperature and energy balance components) are free of substantial trends during this 200-year analysis period (not shown). In a first simulation ("forest world"), forest plant functional types are prescribed on all vegetated areas (reconstructed from observation-based potential vegetation; Pongratz et al., 2008; Ramankutty & Foley, 1999). Thus, in this simulation forests are prescribed also on present-day grasslands, but not in deserts (Figure S2). In subsequent simulations, surface properties are switched from forest to grass values in three out of four grid boxes which we call "change boxes" (Figure S2). These are distributed according to a regular chessboard-like pattern. This strategy allows us to

Table 1
Parameters used in the MPI-ESM Simulations

Plant functional type	$\alpha_{leaf,vis}$	$\alpha_{leaf,nir}$	$z_{0,\Lambda=\infty}$ (m)	$z_{0,\Lambda=0}$ (m)
Forest tropical evergreen	0.03	0.22	2.0	5.0
Forest tropical deciduous	0.04	0.23	1.0	3.0
Forest extratropical evergreen	0.04	0.23	1.0	3.0
Forest extratropical deciduous	0.05	0.26	1.0	3.0
Grass	0.08	0.33	0.005	0.1

Note. Albedo of vegetation-covered surfaces in the visible ($\alpha_{leaf,vis}$) and near-infrared range ($\alpha_{leaf,nir}$); roughness length for vegetation-covered surfaces without leaves ($z_{0,\Lambda=0}$) and with closed canopy ($z_{0,\Lambda=\infty}$). The surface roughness of bare surface (not shown in the table) is set to 0.005 m.

separate local and nonlocal effects, see section 2.3. Specifically, in one simulation ("deforestation") all surface properties are switched from forest to grass values in the change boxes, while in two other simulations, only surface albedo ("albedo") or surface roughness ("roughness") are switched from forest to grass values in the change boxes. The difference between the forest world and one of the other simulations represents the total (local plus nonlocal) biogeophysical effect of switching the respective surface properties.

The choice of deforesting three of four grid boxes (instead of, e.g., deforesting one of four grid boxes) is to some extent arbitrary. However, the local effects within a deforested grid cell, which are the focus of this study, are largely independent of the number of deforested grid cells, concerning both surface temperature and the components of the surface energy balance (see Figures 4a and 4b in Winckler et al., 2017a).

2.3. Isolation of the Simulated Local Effects

The total effects are decomposed into the local and nonlocal effects as follows: In the change boxes, we assume that the total effects are the sum of local and nonlocal effects. In contrast, on nearby no-change boxes, only the nonlocal effects occur. In the change boxes, the nonlocal effects can be obtained by horizontal bilinear interpolation of results from neighboring no-change boxes. Then, the local effects in the change boxes can be calculated as the difference between total and nonlocal effects. Thus, the local effects are the climate signal in the change boxes that goes beyond the signal in surrounding no-change boxes. A detailed explanation of the method is provided in a previous study (Winckler et al., 2017a). This separation of local and nonlocal effects is applied both to changes in surface temperature and to each component of the surface energy balance.

2.4. Comparison of MPI-ESM Results to Observation-Based Data Sets

To assess whether the locally induced changes in surface temperature in the MPI-ESM are plausible, they are compared to various observation-based data sets on the biogeophysical effects of deforestation on surface temperature. These observation-based data sets provide the temperature change upon "potential deforestation" (Li et al., 2016), that is, the changes in radiometric surface temperature that would be caused by a conversion from 100% forests to 0% forests at a given location. The observation-based data sets represent by design only the local effects (Bright et al., 2017; Duveiller et al., 2018b; Li et al., 2015), for example, because they compare temperature between open land and forests (Li et al., 2015), or deforestation-induced temporal changes in temperature (Alkama & Cescatti, 2016) within a moving window of around 50-km length scale. Nonlocal effects from deforestation outside of the moving window would be seen in neighboring locations with and without forests (with and without forest cover change) and are thus by construction not contained in the difference between open land and forests (the difference between deforested and nondeforested locations) that is provided in these data sets. We focus on zonally averaged changes in annual mean surface temperature, the magnitude of the diurnal cycle, and the seasonal cycle. We consider changes in radiometric surface temperature from three satellite-based data sets (Alkama & Cescatti, 2016; Duveiller et al., 2018a; Li et al., 2015), which are biased toward cloud-free conditions, and one semiempirical approach based on Fluxnet observations (Bright et al., 2017). The latter is not restricted to cloud-free conditions but does not provide information about changes in the diurnal amplitude because this data set is not available for daytime and nighttime separately.

The comparison between the MPI-ESM results and these observation-based data sets is challenging. First, the background climate differs across the data sets. While the simulations in the MPI-ESM are subject to a

modeled background climate under preindustrial CO_2 concentrations, the observation-based data sets focus on the more recent past (years 2001–2011 in Bright et al., 2017; 2002–2013 in Li et al., 2015; 2003–2012 in Alkama & Cescatti, 2016; and 2000–2015 in Duveiller et al., 2018b). The difference in background climate could influence the results for the total (local plus nonlocal) biogeophysical effects (Pitman et al., 2011) and also for the locally induced changes in surface temperature (Winckler et al., 2017b) that are analyzed here. However, background climate between preindustrial and present-day did not change strongly enough to substantially change the biogeophysical deforestation effects (e.g., Figure 5 in de Noblet-Ducoudré et al., 2012). Second, the spatial availability of the observation-based data sets differ, see Figure S3. Third, it is challenging to compare the surface temperature in the MPI-ESM with the radiometric surface temperature from the observation-based data sets (Jin & Dickinson, 2010; Winckler, Reick, Luyssaert, et al., 2019). These inconsistencies complicate a fully consistent comparison between the MPI-ESM results and the observation-based data sets. However, the observation-based data sets can still be used to check whether the model results are plausible by assessing whether there is a qualitative match in the response of the annual means, the diurnal amplitude and seasonal response to deforestation.

2.5. Energy Balance Decomposition for the Deforestation-Induced Changes in Surface Temperature

Changes in surface temperature result from the changes in the components of the energy balance (Figure 1). Changes in net shortwave radiation, incoming longwave radiation, sensible heat flux, and latent heat flux are balanced by changes in emitted longwave radiation, which is directly related to surface temperature (T_{surf}) via the Stefan-Boltzmann law. Thus, a change in any of the components of the surface energy balance (W/m^2) can be expressed as a change in surface temperature (K) that would be triggered if only this particular flux was changed and all other surface energy balance components were held constant:

$$\Delta T_{\mathrm{surf}} = \frac{1}{4\sigma\epsilon T_{\mathrm{surf}}^3}(\Delta\text{net shortwave} + \Delta\text{incoming longwave} - \Delta\text{latent} - \Delta\text{sensible}), \tag{2}$$

where σ is the Stefan-Boltzmann constant and ϵ is emissivity and is set to 1. In this way, the surface energy balance decomposition is a useful tool to diagnose the relative contributions of changes in the surface energy balance components to the realized change in surface temperature. Changes in ground heat flux are not considered because we assume that deforestation-induced changes in ground heat flux are negligible on the time scales that we consider in this study. More details on the energy balance decomposition approach can be found elsewhere (e.g., Boisier et al., 2012; Luyssaert et al., 2014).

In the following, we first separate local and nonlocal effects for each existing simulation ("all," "only roughness," and "only albedo"). For each simulation, this separation is performed both for surface temperature and for every component of the surface energy balance (net shortwave radiation, incoming longwave radiation, sensible heat flux, and latent heat flux). Using equation (2), the respective changes are then converted into temperature units.

3. Results

3.1. Simulated Local Effects on Surface Temperature are Largely Consistent With Observations

We compare zonally averaged values from the MPI-ESM simulations with observation-based data. In the simulations, deforestation triggers an annual mean local cooling north of 50°N and a warming further south (Figure 2a), and the surface temperature changes in the MPI-ESM lie within the range of observation-based data sets (see also Winckler, Reick, Lejeune, et al., 2019). The model response is at the lower end of the satellite-based data sets and closer to the Fluxnet-based estimate (Bright et al., 2017), which is free of the cloud bias that is inherent in the satellite-based estimates (Alkama & Cescatti, 2016; Duveiller et al., 2018a; Li et al., 2015). This cloud bias could lead to an overestimation of the local effects on surface temperature in satellite-based estimates (Li et al., 2015). The diurnal cycle of surface temperature is amplified by the local effects of deforestation, both in the model and the satellite-based estimates (Figure 2b). In the low latitudes, the diurnal cycle over grasslands is up to 4 K larger than over forests. Only north of 50°N does the MPI-ESM overestimate the amplification of the diurnal cycle. Concerning the seasonal response to deforestation, qualitatively the model and the observation-based estimates largely agree (Figures 2c and 2d). Both in Northern Hemispheric winter and summer, the locally induced changes in surface temperature in the MPI-ESM closely follow the Fluxnet-based estimate (Bright et al., 2017) and lie at the lower end of the satellite-based estimates (Alkama & Cescatti, 2016; Duveiller et al., 2018a; Li et al., 2015). Only the observations' winter

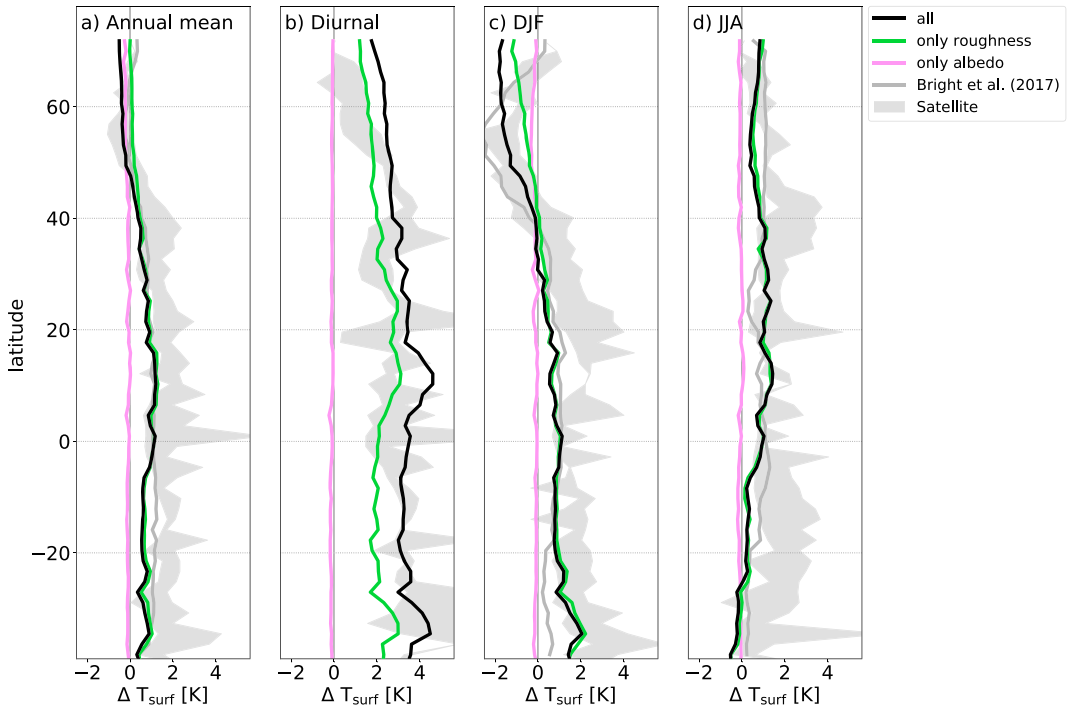

Figure 2. Comparison of the MPI-ESM to observation-based data sets. Deforestation-induced local effects on surface temperature for (a) the annual mean temperature, (b) the amplitude of the diurnal cycle, (c) changes in December to February temperature, (d) changes in June to August temperature. Locally induced changes in surface temperature for (black) changing all surface properties from forest to grass values in the MPI-ESM, and contributions of changing only surface roughness or only surface albedo from tree to grass values. Observation-based data sets from (gray line) Fluxnet (Bright et al., 2017) and (gray shading) remote sensing from satellites (Alkama & Cescatti, 2016; Duveiller et al., 2018a; Li et al., 2015). The data set by Bright et al. (2017) does not provide diurnal values. The zonal averages of MPI-ESM simulation results shown here are obtained exclusively from locations in the zonal band where at least one of the four observation-based data sets provides a value. A separate comparison of the MPI-ESM results to each of the four data sets is shown in Figure S7. The respective maps are shown in Figures S3–S6. JJA = June to August; DJF = December to February.

warming north of 65°N is not captured by the model. The above results are still valid when looking at a one-by-one comparison between the MPI-ESM results and each of the four data sets and obtaining zonal averages for the MPI-ESM only at locations in the zonal band where the respective observation-based data set provides a value (Figure S7).

To summarize, qualitatively the local effects on changes in zonal mean surface temperature in the MPI-ESM are largely in line with the observation-based estimates, both for the annual mean, diurnal, and seasonal response to deforestation. Spatial patterns also align well with observations (Figures S3–S6). Our results for surface temperature in the MPI-ESM are also in qualitative agreement with a study that more comprehensively evaluated the sensitivity of the CLM4.5 model to land cover (Meier et al., 2018), both regarding the sign of local deforestation effects on surface temperature and their seasonality (see their Figure 4). Although the comparison between a model and observations is challenging (section 2) and does not allow to judge whether the model captures all mechanisms correctly, the qualitative agreement between the MPI-ESM results and the observations makes it plausible that the MPI-ESM adequately represents at least the most relevant mechanisms that are responsible for changes in surface temperature that are locally induced by deforestation. This could be evaluated in more detail in future studies.

3.2. Simulated Local Effects are to a Large Extent Caused by Changes in Surface Roughness

3.2.1. Annual Mean

The annual mean changes in surface temperature due to the local effects of deforestation can predominantly be explained by changes in surface roughness in most latitudes (Figure 2a). In contrast, changes in surface albedo locally trigger only small changes in annual mean surface temperature.

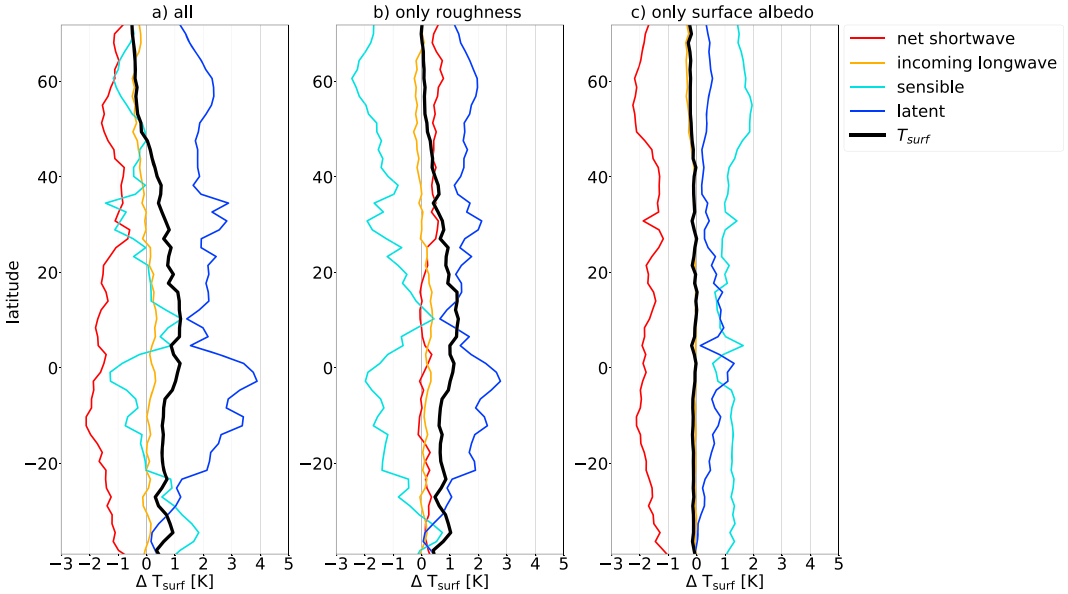

Figure 3. Energy balance decomposition of the locally induced changes of annual mean surface temperature in the MPI-ESM. The lines denote deforestation-induced changes in surface energy balance components for simulations changing (a) all surface properties, (b) only surface roughness, and (c) only surface albedo. Shown is their locally induced impact on surface temperature (same lines as in Figure 2a), net shortwave radiation, incoming longwave radiation, sensible heat, and latent heat, zonally averaged over areas where at least one of the observation-based data sets is available. Note that warming from latent heat is caused by a reduction in evapotranspiration.

A change in any surface property triggers changes in each of the surface energy balance components (Figure 1). Here, we provide an energy balance decomposition (section 2) for the changes in surface temperature that are triggered by changing all surface properties affected by deforestation, changing only surface roughness, and changing only surface albedo (Figure 3). Changes in surface roughness turn out to be a key driver of the local responses of latent and sensible heat fluxes to deforestation (Figures 3a and 3b). A reduction of surface roughness results in less evapotranspiration (less release of latent heat into the atmosphere) over grass compared to forests. If all other surface energy balance components were fixed, this reduction would result in a strong warming (up to 3 K in the inner tropics), but this warming is partly balanced by the increased sensible heat flux, such that changes in surface roughness in the inner tropics locally trigger a warming of around 1 K (Figures 3a and 3b). Changes in surface albedo locally trigger a decrease in net shortwave radiation. This decrease, if all surface energy balance components were kept fixed, would lead to a surface cooling of around 2 K across most latitudes. However, this cooling from decreased net shortwave radiation is largely balanced by the decreased latent and sensible heat fluxes, such that surface temperature barely responds (Figure 3c). Note that while the change in surface roughness is important for the local effects shown here, the change in surface albedo dominates the nonlocal effects in these simulations (Figures S8 and S9).

3.2.2. Diurnal Cycle

Changes in surface roughness are responsible for around two thirds of the amplification of the diurnal cycle in the MPI-ESM throughout the latitudes (Figure 2b). Changes in albedo are negligible for local effects on the diurnal cycle of surface temperature. Approximately one third of the amplification of the diurnal cycle is neither explained by the change in surface roughness nor the change in surface albedo. This residual has to be caused either by changes in evapotranspiration efficiency or by interactions between the three surface properties. Possible mechanisms for the roughness-induced changes in the diurnal amplitude are provided in the discussions section.

3.2.3. Seasonal Cycle

Changes in surface roughness are responsible for most of the deforestation-induced warming in the tropics and in the summer months of the respective hemisphere (Figures 2c and 2d). While some of the boreal winter cooling is caused by changes in the surface albedo, a substantial fraction of the cooling in December to February (DJF) are caused by changes in surface roughness in the MPI-ESM (Figure 2c).

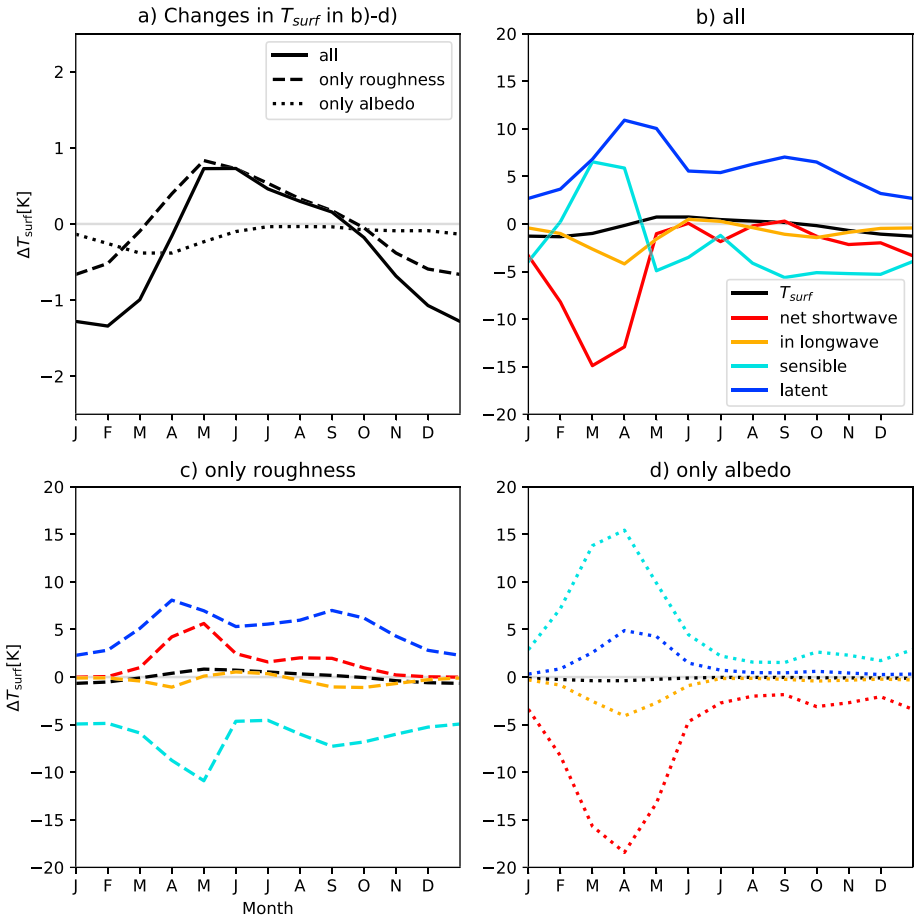

Figure 4. Seasonality of local temperature change due to deforestation and its energy decomposition. Only areas with boreal spring snow cover are considered. (a) Changes in the monthly mean surface temperature (K) due to the local effects of changes in all surface properties (solid line), only surface roughness (dashed line), and only surface albedo (dotted line). These lines are replotted in panels (b)–(d) that show their energy balance decomposition. Panel (b) shows the decomposition for a change in all surface properties, (c) for a change of only surface roughness, and (d) for a change of only surface albedo. The color coding shown in panel (b) is also used in (c) and (d). The values of the energy balance components were converted from watts per square meter into kelvin as described, for example, in the study by Luyssaert et al. (2014). Values are averaged over middle- and high-latitude land areas with spring snow cover (snow cover fraction exceeds 0.5 in March, Figure S10). Note that the values on the *y* axis differ between the plots.

To further investigate the minor importance of surface albedo compared to surface roughness, we consider the deforestation-induced boreal winter cooling and focus on areas where the influence of surface albedo is expected to be the strongest, namely areas with snow cover in spring (Bonan, 2008; here snow cover in March). From the surface property perspective, even in these areas (see Figure S10) the changes in surface roughness are more important for the local cooling in winter (DJF) than the changes in surface albedo (Figure 4a). From the energy balance perspective, the roughness-induced local DJF surface cooling arises from changes in the sensible heat flux (Figure 4c). However, the sensible heat flux appears not to be the dominant driver of the winter cooling when considering changes in all surface properties (Figure 4b) because of concurrent changes in other surface properties. For instance, the cooling from the albedo-induced reduction in net shortwave radiation (especially in April and May; Figure 4d) is balanced by a warming from sensible heat flux. This illustrates that the combination of changes in surface properties influences the surface energy balance in a complex way so that an energy balance decomposition as shown in Figure 4b is not sufficient to infer the responsible surface properties for a change. Instead, factorial experiments are needed to disentangle concurrent changes in the surface energy balance that are caused by changes in the different surface properties.

4. Discussion and Conclusions

Our findings show that in the MPI-ESM, the local effects of deforestation are largely controlled by changes in surface roughness: they dominate the annual and seasonal mean local responses by surface temperature to local deforestation (Figures 2a–2d). On the one hand, our findings are consistent with previous studies that emphasize the importance of surface roughness (e.g., Dickinson & Henderson-sellers, 1988; Khanna & Medvigy, 2014) and even suggested surface roughness as a key driver for local changes in surface temperature (e.g., Lee et al., 2011; Vanden Broucke et al., 2015). On the other hand, the dominance of surface roughness that we find seems to contradict previous studies on the biogeophysical temperature effects of global-scale deforestation in climate models: Some previous studies argued that a reduction of net shortwave radiation at the surface dominates the boreal cooling and a reduction in evapotranspiration is a key driver of the tropical warming (e.g., Bala et al., 2007; Bathiany et al., 2010; Claussen et al., 2001; Devaraju et al., 2015). This apparent discrepancy between our and their results may result from two major differences:

1. The large-scale changes that were imposed in previous studies may result in substantial nonlocal deforestation effects, which may be a reason for the differing conclusions concerning the dominant importance of changes in surface roughness between this and previous climate model studies. The nonlocal effects, which strongly depend on the areal extent and spatial distribution of deforestation, are mingled with the local effects in these simulation and complicate an understanding of the effects of deforestation at a given location. For instance, changes in surface albedo were found to dominate the boreal cooling (Davin & de Noblet-Ducoudré, 2010) and both the surface roughness and evapotranspiration efficiency were found to contribute approximately equally to the tropical warming (Bell et al., 2015; Davin & de Noblet-Ducoudré, 2010; Li et al., 2016). However, changes in surface albedo may mainly affect surface temperature via the nonlocal effects (Winckler, Reick, Lejeune, et al., 2019), and further changes in evapotranspiration efficiency could trigger changes in cloudiness and precipitation (Ban-Weiss et al., 2011), which could affect also locations without deforestation. For the particular areal extent and spatial distribution of the simulations used in this study, the nonlocal effects on surface temperature and the surface energy balance decomposition thereof is given in Figure S8. When looking at the total (local plus nonlocal) biogeophysical effects, indeed, surface albedo largely dominates the response of the MPI-ESM (Figure S9).
2. In our simulations in which only one single surface property is switched, the influence of the surface properties on the local effects can be assessed *directly* while many previous studies inferred the mechanisms *indirectly* via an analysis of deforestation-induced changes in the components of the surface energy balance (e.g., net shortwave radiation or latent heat; e.g., Claussen et al., 2001; Brovkin et al., 2009; Devaraju et al., 2015; Duveiller et al., 2018b). If the latter is done, surface albedo is intuitively assigned a large relevance because it is the surface property that is associated with the large reduction in net shortwave radiation following deforestation. However, it may easily be overlooked that this reduction in shortwave radiation can locally be largely compensated by reductions in the turbulent heat fluxes, such that the overall influence of changes in surface albedo on the local effects on surface temperature is small. On the other hand, for surface roughness there is no such compensating mechanism, and this is why changes the local effects on surface temperature in the MPI-ESM are dominated by changes in surface roughness.

Note that our conclusion, that the surface roughness is more important than surface albedo for the local effects, may depend on the parametrizations of surface albedo and surface roughness in the respective climate model because the temperature change from albedo reduction is the result of two counteracting mechanisms (change in surface net radiation and response of the latent and sensible heat fluxes) whose net result may depend on subtle details of the model formulation. The deforestation-induced change in surface albedo in the MPI-ESM is on the lower end of a range of climate models and lower than in observations (Boisier et al., 2013). Further studies may investigate if our conclusions are also valid in other climate models with a different representation of surface albedo and surface roughness.

In contrast to the climate model studies, satellite-based studies (Alkama & Cescatti, 2016; Duveiller et al., 2018b; Li et al., 2015) only include changes in surface temperature from local effects, so their results could conceptually be compared to our local effects. The satellite-based studies adopted the argumentation from the climate model studies (e.g.,Bathiany et al., 2010; Claussen et al., 2001; Devaraju et al., 2015) that a reduction of net shortwave radiation at the surface dominates the boreal cooling and a reduction in evapotranspiration dominates the tropical warming. It was argued that in boreal regions, the surface cooling is correlated to snow frequency (Li et al., 2015) and thus surface albedo. However, our findings hint to a pos-

sible correlation without causation: we find that the local effects of changes in surface roughness cool the surface in the high northern latitudes during winter (Figure 4), that is, exactly in cases with a potentially high snow frequency. Our results suggest that surface roughness could dominate this deforestation-induced local cooling. During high-latitude winter, the surface is generally cooler than the atmosphere aloft. Thus, the responsible mechanism for the roughness-induced northern winter cooling could be similar to the hypothesis that was given for the nighttime cooling following deforestation (Lee et al., 2011; Vanden Broucke et al., 2015) and corresponding empirical evidence (Schultz et al., 2017). These studies argued that the high surface roughness of forests allows the surface to dissipate energy into the atmosphere during daytime conditions, while during nighttime the high surface roughness of forests allows the surface to gain energy from the warmer atmosphere aloft (Schultz et al., 2017; Vanden Broucke et al., 2015). Accordingly, deforestation, which reduces roughness, reduces daytime surface cooling and nighttime surface warming, leading to a cooler surface at nights or—in analogy—in winter.

While we separated the effects of changing only surface albedo and only surface roughness, we did not separate the effects of only changing evapotranspiration efficiency. A clean isolation of changes in evapotranspiration efficiency is technically challenging because this surface property is a complex composition of various land surface characteristics, for example, rooting depth, canopy water holding capacity, photosynthesis, and stomatal conductance (Davin & de Noblet-Ducoudré, 2010), and some of these variables are not simple parameters but calculated dynamically during a model run. Previous studies (Bell et al., 2015; Davin & de Noblet-Ducoudré, 2010; Li et al., 2016), solved this problem by changing both surface albedo and surface roughness from grass to forest values and interpreting the signal from evapotranspiration efficiency as the difference to the "forest state." However, this approach does not yield the isolated evapotranspiration efficiency but instead still includes all interactions (between evapotranspiration efficiency and surface albedo, evapotranspiration efficiency and surface roughness, and interactions between all three surface properties) when changing together with the two other surface properties (Stein & Alpert, 1993). Because we do not perform a simulation in which we only change evapotranspiration efficiency, we can only conclude that changes in surface roughness in the MPI-ESM are *sufficient* to explain local changes in surface temperature, but we cannot conclude that they are *necessary*. A further limitation of our study is that we use a model with a resolution of around 200km, which means that we cannot investigate the influence of deforestation-induced mesoscale circulations (e.g., Roy & Avissar, 2002). Resolving such mesoscale circulations and associated changes in cloud cover and precipitation would require simulations at a resolution of 32 km or smaller (Khanna et al., 2018).

As demonstrated here, the interpretation of the mechanisms underlying the local effects of deforestation depends crucially on the perspective. Concerning deforestation in the low latitudes, from the surface energy flux perspective, the local warming in the MPI-ESM seems to be dominated by the reduction of evapotranspiration. From the surface properties perspective, the changes in surface temperature and evapotranspiration are dominated by changes in surface roughness. Concerning deforestation in the high latitudes, from the surface energy balance perspective, the local cooling in the MPI-ESM seems to be dominated by the reduction in surface net shortwave radiation. However, this does not imply that surface albedo is the surface property that is responsible for most of the overall cooling—we showed that the reduction in net shortwave radiation is locally compensated in its temperature effect by a reduction in losses of latent and sensible heat. Instead, even in areas with high spring snow cover where the influence of surface albedo would be expected to be strong, the local cooling in the MPI-ESM can to a large part be explained by the reduction in surface roughness. Thus, this study reconciles two different views on the mechanisms underlying the local effects of deforestation.

Acknowledgments
Our simulations were performed at the German Climate Computing Center (DKRZ). This research was supported by the Deutsche Forschungsgemeinschaft (Grant PO1751). R. M. B. was supported with funding provided by the Research Council of Norway (250113/F20). We want to thank all groups who provided observation-based data. Data, scripts used in the analysis, and other supporting information that may be useful in reproducing the authors work can be found in http://hdl.handle.net/21.11116/0000-0003-9DEC-3 website.

References

Alkama, R., & Cescatti, A. (2016). Biophysical climate impacts of recent changes in global forest cover. *Science*, *351*, 600–604. https://doi.org/10.1126/science.aac8083

Anderson, R. G., Canadell, J. G., Randerson, J. T., Jackson, R. B., Hungate, B. A., Baldocchi, D. D., et al. (2010). Biophysical considerations in forestry for climate protection. *Frontiers in Ecology and the Environment*, *9*(3), 174–182. https://doi.org/10.1890/090179

Avissar, R., & Werth, D. (2005). Global hydroclimatological teleconnections resulting from tropical deforestation. *Journal of Hydrometeorology*, *6*(2), 134–145.

Badger, A. M., & Dirmeyer, P. A. (2016). Remote tropical and sub-tropical responses to Amazon deforestation. *Climate Dynamics*, *46*(9), 3057–3066. https://doi.org/10.1007/s00382-015-2752-5

Bala, G., Caldeira, K., Wickett, M., Phillips, T. J., Lobell, D. B., Delire, C., & Mirin, A. (2007). Combined climate and carbon-cycle effects of large-scale deforestation. *Proceedings of the National Academy of Sciences*, *104*(16), 6550–6555. https://doi.org/10.1073/pnas.0608998104

Ban-Weiss, G. A., Bala, G., Cao, L., Pongratz, J., & Caldeira, K. (2011). Climate forcing and response to idealized changes in surface latent and sensible heat. *Environmental Research Letters*, *6*, 1–8. https://doi.org/10.1088/1748-9326/6/3/034032

Bathiany, S., Claussen, M., Brovkin, V., Raddatz, T., & Gayler, V. (2010). Combined biogeophysical and biogeochemical effects of large-scale forest cover changes in the MPI Earth system model. *Biogeosciences*, *7*, 1383–1399. https://doi.org/10.5194/bg-7-1383-2010

Bell, J. P., Tompkins, A. M., Bouka-Biona, C., & Seidou Sanda, I. (2015). A process-based investigation into the impact of the Congo basin deforestation on surface climate. *Journal of Geophysical Research: Atmospheres*, *120*, 5721–5739. https://doi.org/10.1002/2014JD022586

Berg, A., Findell, K., Lintner, B., Giannini, A., Seneviratne, S. I., Lorenz, R., et al. (2016). Land-atmosphere feedbacks amplify aridity increase over land under global warming. *Nature Climate Change*, 1–7. https://doi.org/10.1038/NCLIMATE3029

Boisier, J. P., de Noblet-Ducoudré, N., & Ciais, P. (2013). Inferring past land use-induced changes in surface albedo from satellite observations: a useful tool to evaluate model simulations. *Biogeosciences*, *10*, 1501–1516. https://doi.org/10.5194/bg-10-1501-2013

Boisier, J. P., de Noblet-Ducoudré, N., & Ciais, P. (2014). Historical land-use-induced evapotranspiration changes estimated from present-day observations and reconstructed land-cover maps. *Hydrology and Earth System Sciences*, *18*, 3571–3590. https://doi.org/10.5194/hess-18-3571-2014

Boisier, J. P., de Noblet-Ducoudré, N., Pitman, A. J., Cruz, F. T., Delire, C., van den Hurk, B. J. J. M., et al. (2012). Attributing the impacts of land-cover changes in temperate regions on surface temperature and heat fluxes to specific causes: Results from the first LUCID set of simulations. *Journal of Geophysical Research*, *117*, D12116. https://doi.org/10.1029/2011JD017106

Bonan, G. B. (2008). Forests and climate change: Forcings, feedbacks, and the climate benefits of forests. *Science*, *320*, 1444–1449. https://doi.org/10.1126/science.1155121

Bright, R. M., Davin, E. L., O'Halloran, T. L., Pongratz, J., Zhao, K., & Cescatti, A. (2017). Local temperature response to land cover and management change driven by non-radiative processes. *Nature Climate Change*, *7*, 296–302. https://doi.org/10.1038/nclimate3250

Brovkin, V., Boysen, L., Arora, V. K., Boisier, J. P., Cadule, P., Chini, L., et al. (2013). Effect of anthropogenic land-use and land-cover changes on climate and land carbon storage in CMIP5 projections for the twenty-first century. *Journal of Climate*, *26*, 6859–6881. https://doi.org/10.1175/JCLI-D-12-00623.1

Brovkin, V., Boysen, L., Raddatz, T., Gayler, V., Loew, A., & Claussen, M. (2013). Evaluation of vegetation cover and land-surface albedo in MPI-ESM CMIP5 simulations. *Journal of Advances in Modeling Earth Systems*, *5*, 48–57. https://doi.org/10.1029/2012MS000169

Brovkin, V., Raddatz, T., Reick, C. H., Claussen, M., & Gayler, V. (2009). Global biogeophysical interactions between forest and climate. *Geophysical Research Letters*, *36*, L07405. https://doi.org/10.1029/2009GL037543

Burakowski, E., Ouimette, A., Lepine, L., Novick, K., Ollinger, S., Zarzycki, C., & Bonan, G. (2018). The role of surface roughness, albedo, and Bowen ratio on ecosystem energy balance in the Eastern United States. *Agricultural and Forest Meteorology*, *249*, 367–376. https://doi.org/10.1016/j.agrformet.2017.11.030

Charney, J., Quirk, W. J., Chow, S.-H., & Kornfield, J. (1977). A comparative study of the effects of albedo change on drought in semi-arid regions. *Journal of the Atmospheric Sciences*, *34*, 1366–1385.

Chen, L., & Dirmeyer, P. A. (2016). Adapting observationally based metrics of biogeophysical feedbacks from land cover/land use change to climate modeling. *Environmental Research Letters*, *11*(3), 034002. https://doi.org/10.1088/1748-9326/11/3/034002

Claussen, M. (1995). Flux aggregation at large scales: On the limits of validity of the concept of blending height. *Journal of Hydrology*, *166*, 371–382.

Claussen, M., Brovkin, V., & Ganopolski, A. (2001). Biogeophysical versus biogeochemical feedbacks of large-scale land cover change. *Geophysical Research Letters*, *28*, 1011–1014.

Davin, E. L., & de Noblet-Ducoudré, N. (2010). Climatic impact of global-scale deforestation: Radiative versus nonradiative processes. *Journal of Climate*, *23*(1), 97–112. https://doi.org/10.1175/2009JCLI3102.1

Davin, E., Seneviratne, S., Ciais, P., Olioso, A., & Wang, T. (2014). Preferential cooling of hot extremes from cropland albedo management. *Proceedings of the National Academy of Sciences*, *111*(27), 9757–9761. https://doi.org/10.1073/pnas.1317323111

de Noblet-Ducoudré, N., Boisier, J.-P., Pitman, A., Bonan, G. B., Brovkin, V., Cruz, F., et al. (2012). Determining robust impacts of land-use-induced land cover changes on surface climate over North America and Eurasia: Results from the first set of LUCID experiments. *Journal of Climate*, *25*, 3261–3281. https://doi.org/10.1175/JCLI-D-11-00338.1

Devaraju, N., Bala, G., & Modak, A. (2015). Effects of large-scale deforestation on precipitation in the monsoon regions: Remote versus local effects. *Proceedings of the National Academy of Sciences*, *112*, 3257–3262. https://doi.org/10.1073/pnas.1423439112

Devaraju, N., Quesada, B., Bala, G., & de Noblet-Ducoudré, N. (2018). Quantifying the relative importance of direct and indirect biophysical effects of deforestation on surface temperature and teleconnections. *Journal of Climate*, *31*(10), 3811–3829. https://doi.org/10.1175/JCLI-D-17-0563.1

Dickinson, R. E., Henderson-Sellers, A., & Kennedy, P. J. (1993). Biosphere-Atmosphere Transfer Scheme (BATS) version le as coupled to the NCAR Community Climate Model (Technical Note (August)): NCAR.

Dickinson, R. E., & Henderson-sellers, A. (1988). Modelling tropical deforestation: A study of GCM land-surface parametrizations. *Quarterly Journal of the Royal Meteorological Society*, *114*, 439–462.

Duveiller, G., Forzieri, G., Robertson, E., Li, W., Georgievski, G., Lawrence, P., et al. (2018). Biophysics and vegetation cover change: A process-based evaluation framework for confronting land surface models with satellite observations. *Earth System Science Data*, *10*, 1265–1279.

Duveiller, G., Hooker, J., & Cescatti, A. (2018a). A dataset mapping the potential biophysical effects of vegetation cover change. *Scientific Data*, *5*, 1–15. https://doi.org/10.1038/sdata.2018.14

Duveiller, G., Hooker, J., & Cescatti, A. (2018b). The mark of vegetation change on Earth's surface energy balance. *Nature Communications*, *9*(1), 1–12. https://doi.org/10.1038/s41467-017-02810-8

Giorgetta, M. A., Roeckner, E., Mauritsen, T., Bader, J., Crueger, T., Esch, M., et al. (2013). The atmospheric general circulation model ECHAM6—Model description (Tech. Rep. No. 135). Hamburg: Max-Planck-Institute for Meteorology.

Jin, M., & Dickinson, R. E. (2010). Land surface skin temperature climatology: Benefitting from the strengths of satellite observations. *Environmental Research Letters*, *5*(4), 1–13. https://doi.org/10.1088/1748-9326/5/4/044004

Juang, J. Y., Katul, G., Siqueira, M., Stoy, P., & Novick, K. (2007). Separating the effects of albedo from eco-physiological changes on surface temperature along a successional chronosequence in the southeastern United States. *Geophysical Research Letters*, *34*, L21408. https://doi.org/10.1029/2007GL031296

Khanna, J., & Medvigy, D. (2014). Strong control of surface roughness variations on the simulated dry season regional atmospheric response to contemporary deforestation in Rondônia, Brazil. *Journal of Geophysical Research: Atmospheres*, *119*, 67–78. https://doi.org/10.1002/2014JD022278

Khanna, J., Medvigy, D., Fisch, G., & de Araujo Tiburtino Neves, T. T. (2018). Regional Hydroclimatic Variability due to Contemporary Deforestation in Southern Amazonia and Associated Boundary Layer Characteristics. *Journal of Geophysical Research: Atmospheres*, *123*, 3993–4014. https://doi.org/10.1002/2017JD027888

Khanna, J., Medvigy, D., Fueglistaler, S., & Walko, R. (2017). Regional dry-season climate changes due to three decades of Amazonian deforestation. *Nature Climate Change*, *7*(3), 200–204. https://doi.org/10.1038/nclimate3226

Le Quéré, C., Andrew, R. M., Friedlingstein, P., Sitch, S., Pongratz, J., Manning, A. C., et al. (2018). Global carbon budget 2017. *Earth System Science Data*, *10*(1), 405–448. https://doi.org/10.5194/essd-10-405-2018

Lee, X., Goulden, M. L., Hollinger, D. Y., Barr, A., Black, T. A., Bohrer, G., et al. (2011). Observed increase in local cooling effect of deforestation at higher latitudes. *Nature*, *479*, 384–387. https://doi.org/10.1038/nature10588

Li, Y., de Noblet-Ducoudré, N., Davin, E. L., Zeng, N., Motesharrei, S., Li, S. C., & Kalnay, E. (2016). The role of spatial scale and background climate in the latitudinal temperature response to deforestation. *Earth System Dynamics Discussions*, *7*, 167–181. https://doi.org/10.5194/esdd-6-1897-2015

Li, Y., Zhao, M., Mildrexler, D. J., Motesharrei, S., Mu, Q., Kalnay, E., et al. (2016). Potential and actual impacts of deforestation and afforestation on land surface temperature. *Journal of Geophysical Research: Atmospheres*, *121*, 14,372–14,386. https://doi.org/10.1002/2016JD024969

Li, Y., Zhao, M., Motesharrei, S., Mu, Q., Kalnay, E., & Li, S. (2015). Local cooling and warming effects of forests based on satellite observations. *Nature Communications*, *6*, 1–8. https://doi.org/10.1038/ncomms7603

Liao, W., Rigden, A. J., Li, D., Sciences, P., & Li, D. (2018). Attribution of local temperature response to deforestation. *Journal of Geophysical Research: Biogeosciences*, *123*, 1572–1587. https://doi.org/10.1029/2018JG004401

Loew, A., Stacke, T., Dorigo, W., de Jeu, R., & Hagemann, S. (2013). Potential and limitations of multidecadal satellite soil moisture observations for selected climate model evaluation studies. *Hydrology and Earth System Sciences*, *17*, 3523–3542. https://doi.org/10.5194/hess-17-3523-2013

Lorenz, R., Pitman, A. J., & Sisson, Scotta (2016). Does Amazonian deforestation cause global effects; can we be sure? *Journal of Geophysical Research: Atmospheres*, *121*, 5567–5584. https://doi.org/10.1002/2015JD024357

Luyssaert, S., Jammet, M., Stoy, P. C., Estel, S., Pongratz, J., Ceschia, E., et al. (2014). Land management and land-cover change have impacts of similar magnitude on surface temperature. *Nature Climate Change*, *4*, 389–393. https://doi.org/10.1038/NCLIMATE2196

Meier, R., Davin, E. L., Lejeune, Q., Hauser, M., Li, Y., Martens, B., et al. (2018). Evaluating and improving the Community Land Model's sensitivity to land cover. *Biogeosciences*, *15*, 4731–4757.

Otto, J., Raddatz, T., & Claussen, M. (2011). Strength of forest-albedo feedback in mid-Holocene climate simulations. *Climate of the Past*, *7*, 1027–1039. https://doi.org/10.5194/cp-7-1027-2011

Pitman, A. J., Avila, F. B., Abramowitz, G., Wang, Y. P., Phipps, S. J., & de Noblet-Ducoudré, N. (2011). Importance of background climate in determining impact of land-cover change on regional climate. *Nature Climate Change*, *1*, 472–475. https://doi.org/10.1038/nclimate1294

Pitman, A. J., de Noblet-Ducoudré, N., Cruz, F. T., Davin, E. L., Bonan, G. B., Brovkin, V., et al. (2009). Uncertainties in climate responses to past land cover change: First results from the LUCID intercomparison study. *Geophysical Research Letters*, *36*, L14814. https://doi.org/10.1029/2009GL039076

Polcher, J. (1995). Polcher2015.pdf. *Journal of the Atmospheric Sciences*, *52*(17), 3143–3161.

Pongratz, J., Reick, C. H., Raddatz, T., & Claussen, M. (2008). A reconstruction of global agricultural areas and land cover for the last millennium. *Global Biogeochemical Cycles*, *22*, GB3018. https://doi.org/10.1029/2007GB003153

Ramankutty, N., & Foley, J. A. (1999). Estimating historical changes in global land cover: Croplands from 1700 to 1992. *Global Biogeochemical Cycles*, *13*(4), 997–1027.

Rigden, A., & Li, D. (2017). Attribution of surface temperature anomalies induced by land use and land cover changes. *Geophysical Research Letters*, *44*, 6814–6822. https://doi.org/10.1002/2017GL073811

Roy, S. B., & Avissar, R. (2002). Impact of land use/land cover change on regional hydrometeorology in Amazonia. *Journal of Geophysical Research*, *107*(D20), 1–12. https://doi.org/10.1029/2000JD000266

Schultz, N. M., Lawrence, P. J., & Lee, X. (2017). Global satellite data highlights the diurnal asymmetry of the surface temperature response to deforestation. *Journal of Geophysical Research: Biogeosciences*, *122*, 903–917. https://doi.org/10.1002/2016JG003653

Seneviratne, S. I., Phipps, S. J., Pitman, A. J., Hirsch, A. L., Davin, E. L., Donat, M. G., et al. (2018). Land radiative management as contributor to regional-scale climate adaptation and mitigation. *Nature Geoscience*, *11*(2), 88–96. https://doi.org/10.1038/s41561-017-0057-5

Seneviratne, S. I., Wilhelm, M., Stanelle, T., Hagemann, S., Berg, A., Cheruy, F., et al. (2013). Impact of soil moisture-climate feedbacks on CMIP5 projections: First results from the GLACE-CMIP5 experiment. *Geophysical Research Letters*, *40*, 5212–5217. https://doi.org/10.1002/grl.50956

Stein, U., & Alpert, P. (1993). Factor separation in numerical simulations. *Journal of the Atmospheric Sciences*, *50*(14), 2107–2115.

Sud, Y. C., Shukla, J., & Mintz, Y. (1988). Influence of land surface roughness on atmospheric circulation and precipitation: A sensitivity study with a general circulation model. *Journal of Applied Meteorology*, *27*, 1036–1054.

Sud, Y. C., & Smith, W. E. (1985). The influence of surface roughness of deserts on the July circulation. *Boundary-Layer Meteorology*, *33*, 15–49.

Teuling, A. J., Taylor, C. M., Meirink, J. F., Melsen, L. A., Miralles, D. G., van Heerwaarden, C. C., et al. (2017). Observational evidence for cloud cover enhancement over western European forests. *Nature Communications*, *8*, 14065. https://doi.org/10.1038/ncomms14065

Thiery, W., Davin, E. L., Lawrence, D. M., Hirsch, A. L., Hauser, M., & Seneviratne, S. I. (2017). Present-day irrigation mitigates heat extremes. *Journal of Geophysical Research: Atmospheres*, *122*, 1403–1422. https://doi.org/10.1002/2016JD025740

Vanden Broucke, S., Luyssaert, S., Davin, E. L., Janssens, I., & Lipzig, N. (2015). New insights in the capability of climate models to simulate the impact of LUC based on temperature decomposition of paired site observations. *Journal of Geophysical Research: Atmospheres*, *120*, 5417–5436. https://doi.org/10.1002/2015JD023095

Winckler, J., Reick, C. H., Lejeune, Q., & Pongratz, J. (2019). Nonlocal effects dominate the global mean surface temperature response to the biogeophysical effects of deforestation. *Geophysical Research Letters*, *46*, 745–755. https://doi.org/10.1029/2018gl080211

Winckler, J., Reick, C. H., Luyssaert, S., Cescatti, A., Stoy, P. C., Lejeune, Q., et al. (2019). Different response of surface temperature and air temperature to deforestation in climate models. *Earth System Dynamics*, *10*, 473–484. https://doi.org/10.5194/esd-10-473-2019

Winckler, J., Reick, C. H., & Pongratz, J. (2017a). Robust identification of local biogeophysical effects of land-cover change in a global climate model. *Journal of Climate*, *30*(3), 1159–1176. https://doi.org/10.1175/JCLI-D-16-0067.1

Winckler, J., Reick, C. H., & Pongratz, J. (2017b). Why does the locally induced temperature response to land cover change differ across scenarios? *Geophysical Research Letters*, *44*, 3833–3840. https://doi.org/10.1002/2017GL072519

Zhang, L., Dobslaw, H., Stacke, T., Dill, R., Thomas, M., & Potsdam, C. (2017). Validation of terrestrial water storage variations as simulated by different global numerical models with GRACE satellite observations. *Hydrology and Earth System Sciences*, *21*, 821–837. https://doi.org/10.5194/hess-21-821-2017